Spectropolarimetric studies of atmospheric aerosols

A.A. Isakov, S.L. Begunov, S.A. Golovyatinskii, and A.V. Tikhonov

Institute of Atmospheric Physics, Russian Academy of Sciences, Moscow
Received March 30, 1999

A spectropolarimeter for the investigation of natural and smoke aerosols is described. The instrument allows one to measure the scattering phase function and linear polarization of scattered light at three angles 45°, 90°, and 135° in the spectral region 0.4–0.75 μm with quasicontinuous scanning of the spectrum. Some measurement results are presented, obtained under conditions of high transparency of the atmosphere (meteorological visibility range $S_m = 30$ km) and in damp haze ($S_m = 5$ km). From these optical characteristics the inverse problem is solved, i.e., the particle-volume size distributions are reconstructed and the complex refractive index of the particle material and the dependence of the condensation activity of the particles on radius are estimated.

Introduction

The extended use and testing to which nephelometers and polarimeters for studying atmospheric aerosols have been put over the years provide a basis, upon which to distinguish the stages that have configured the formation of present-day measurement techniques and the currently available instrumentation. Outside the Soviet Union during the 60's and 70's, a sizable amount of experimental material was accumulated on trends in the variability of light scattering by atmospheric aerosols, with the regime in which the devices operated at one wavelength predominating (this was usually $\lambda \approx 0.5$ μm, which figured in the first models of atmospheric optics) and the authors strove to record in the greatest detail possible the dependence on the angle φ of the components of the aerosol scattering matrix $D_{ik}(\varphi)$ (Ref. 1). Spectral dependences were recorded only for the attenuation coefficient $\varepsilon(\lambda)$ on ground-level and inclined paths since a knowledge of the trends of its variations is required to solve many applied problems. The large size of the first Stokes polarimeters and the laboriousness of the measurements motivated many researchers to build more compact and simpler devices recording only the scattering phase function D_{11} or its polarization components.[2]

A statistical analysis of large data sets[1,12] has shown that to within the measurement errors the angular dependence of the matrices can be represented with the help of two to five of its values measured at characteristic angles. This made it possible to do without cumbersome scanners and go over to a setup with several synchronously operating photometers,[3] which in turn has significantly shortened the measurement time.

At roughly the same time the idea arose of solving the inverse problem, i.e., retrieving the microphysical characteristics of the aerosol from its scattering matrix. This idea was most completely formulated by G.V. Rozenberg.[4] He was the first to clearly formulate the problem of the simultaneous independent determination of both the parameters of the aerosol particle size distribution and also the real and imaginary parts of the refractive index of the particle material. He was also the first to show that to solve this problem it is necessary to have a knowledge of the spectral dependence of the components of the scattering matrix because single-wavelength measurements carry information about the particle size distribution only over a narrow range.

In parallel with the development of computing technology, several model calculations appeared along with light-scattering tables, which were convenient for analysis.[5] Together with approximate calculations for the so-called "soft particles," i.e., particles with refractive index n close to unity, analysis of the tables pointed to an unavoidable defect of measuring only the scattering phase function D_{11} (from the viewpoint of solving the inverse problem), namely the fact that its dependence on the scattering angle φ is determined by the product of the relative size of the particle $\rho = 2\pi a/\lambda$ (here a is the particle radius) and the quantity $(n-1)^{\alpha(\varphi)}$. The dependence of the exponent $\alpha(\varphi)$ on the scattering angle is quite weak, thus for $\varphi = 45°$ $\alpha \approx 0.5$. In other words, it is difficult to determine independently the size of the particle and its refractive index from the angular dependence of D_{11}. To a lesser extent this also applies to the second component of the scattering matrix—the degree of linear polarization of the scattered light f_{21} since the polarization components of the phase function have a different sensitivity to variations of ρ and n. It would be very useful to measure the component f_{43} of the scattering matrix, i.e., the degree of ellipticity of the polarization, but such measurements require a substantial elaboration of the apparatus, and, what is even more important, they narrow its spectral range since a quarter-wave plate, being an indispensable element of the technique, maintains its properties only over a narrow spectral range.

Thus, attempts to optimize the apparatus were made: it was decided that the design of the device should include two to four characteristic scattering angles and three to four working wavelengths with the

0235-6880/99/06 537-06 $02.00

measured quantities being the scattering phase function and the degree of linear polarization. As an example we may cite the commercially available device FAN, which after the necessary adjustments has been used successfully at the Institute of Atmospheric Optics in Tomsk for ground-level measurements and has also been incorporated in the instrument suite of their airborne laboratory.[13]

These arguments lay at the basis of the measurement technique of the four-wavelength spectropolarimeter that served as the prototype for the device described below. The experience gained from its use, in particular during the multicomponent smoke experiment conducted within the context of the program "nuclear winter,"[6] clearly showed that in a number of cases an anomalous spectral dependence is observed in the optical characteristics of the aerosol. In studies of such anomalies a more detailed spectral scanning of the matrix components D_{ik} would be useful. In 1988 a mockup version of such a device was built incorporating an illuminator based on a ground-level monochromator.[7] The measurement technique realized in the device described below was developed on the basis of this mockup. In the present paper we have deliberately focused our attention on methodological questions by choosing for analysis of the potential role spectropolarimetry can play in studies of the microphysics of aerosols several sample records from a data set obtained over the course of four months (May to September, 1993). We think that additional analysis of these results which implements the indicated algorithms and includes a statistical analysis may serve as a basis for subsequent work.

Description of the device

The design of the device is analogous to that described in Ref. 6. The illuminator of the device is based on a MSD−1 monochromator. This choice is motivated by its small size and high light power (relative aperture 1:3.5). A KGM incandescent lamp serves as the light source. Its flux is focused by a parabolic mirror onto the entrance slit of the monochromator. The spectral resolution of the device with the slits completely open is 15 nm. Extinction of superfluous orders is achieved with the aid of a ZhS10 yellow cutoff filter switched on with the help of a solenoid during computer-controlled scanning. The illuminator beam is modulated in intensity at a frequency around 1000 Hz and in the orientation of the polarization plane with a frequency around 15 Hz. Modulation in amplitude with subsequent synchronous detection decreases the vulnerability of the device to stray light through the air-intake channel, and polarization modulation makes it possible in a comparatively simple way to record the second component of the scattering matrix—the degree of linear polarization of the scattered light. The exit lens, positioned so that the monochromator slit is located at its focus, forms a quasiparallel beam with diameter around 3 cm. The polarization modulator is a polaroid with an orientation sensor, which is rotated at a frequency around 15 Hz. The polarization recording scheme is analogous to that described in Ref. 6. The sensor forms two sequences of short gate pulses, one of which is referenced to the times when the polarization plane of the polaroid is parallel to the scattering plane in the polarimeter, and the other, to when it is perpendicular. Gate-controlled switches determine the intensity of the scattered light for the two mutually perpendicular orientations of the polaroid, as is required in the classical determination of the degree of linear polarization.

The stream of sampled air passes along the vertical axis of the working chamber, and the scattering plane is horizontal. Three identical photometers based on FEU−79 photomultipliers are mounted at scattering angles $\varphi = 45$, 90, and 135°. The polarimeter is equipped with a low-temperature heater for heating the sampled air in order to investigate the so-called condensation activity of the atmospheric aerosol. It heats the aerosol at the entrance to the chamber by 15–20 °C, whereupon the relative humidity of the air in the chamber is decreased to $Rh \approx 15$–20% and the device records scattering by the dry residue of the particles. The temperature sensors monitor this component at the entrance to the air-intake channel and at the output of the heater so that knowing the absolute humidity of the sampled air, it is easy to calculate the drop in the relative humidity ΔRh from the corresponding temperature drop ΔT.

The operational calibration of the device against a reference scatterer is also analogous to that described in Ref. 6. Upon a command from the computer this scatterer (a fluoroplastic screen) is introduced into the fields of view of the photometers. During absolute calibration of the device, its signal is referenced to the calibration constants and from that point on serves as an operational secondary standard. Simultaneously, this reference scatterer made it possible to carry out a polarization calibration of the device. The point here is that grating monochromators frequently polarize the transmitted radiation, where the degree of this polarization δ varies strongly (from $\approx 5\%$ to 50%) from sample to sample. Therefore, at the output of the polarization modulator, the beam intensity I_1 will vary according to the following law as a function of the rotation angle θ of the polaroid:

$$I_1 = I_0 [1 + \delta(1 - \sin\theta)]. \quad (1)$$

The beam intensity I_1 varies synchronously with rotation of the polaroid, where the amplitude of these variations depends on the degree of intrinsic polarization of the monochromator δ, which in turn depends strongly on the light wavelength. Thus, to measure the degree of polarization of the scattered light it is necessary to know at least I_1 at the times when the polarization plane of the polaroid is parallel and

perpendicular to the scattering plane, i.e., at the gate times of the polarization modulator. This circumstance made it possible to use the same reference scatterer for polarization calibration of the device as for calibration of its sensitivity. The fluoroplastic screen is insensitive to the polarization state of the illuminating beam, and the light transmitted by it is proportional to I_1. Recording the spectral dependence of the beam intensities when the polarization plane is perpendicular $[I_1(\lambda, \varphi)]$ and parallel $[I_2(\lambda, \varphi)]$ to the scattering plane for the screen in the standard recording regime for all three photometers, we obtain a tool for polarization calibration.

Alignment of the sensors of the polarization modulator is achieved by a frequently used technique: with the light trap at the output of the chamber removed, the illuminator beam is reflected by a plane-parallel glass plate mounted at the "rewster angle on a special table with a goniometer, and generation of the sensor pulse is referenced to total extinction of the reflected beam.

Spectral calibration of the device is performed with the aid of a reference reflecting screen spray-coated with a layer of magnesium oxide. In analogy with polarization calibration, the signals $F_1(\lambda, \varphi)$ and $F_2(\lambda, \varphi)$ are recorded for the reference screen.

Absolute calibration is performed by the method described in Ref. 6. The instrumentation of the device includes a sedimentation tube for studying smoke aerosols. It is mounted in the working chamber so that its longitudinal axis coincides with the beam axis. When working with smoke aerosols, the chamber and tube are filled with the investigated smoke. A photodetector is mounted at the bottom of the sedimentation tube. This photodetector records the intensity I_1 for the empty chamber and the intensity I_2 when the chamber is filled with smoke. In the latter case the extinction coefficient τ of the column of smoke is calculated from the beam attenuation as

$$\tau = \ln(I_1/I_2). \qquad (2)$$

As a sample scatterer we also used rosin vapor as in Ref. 6 since it is easy to determine the scattering phase function D for rosin smoke in terms of the scattering coefficient $\sigma = \tau/L$, where L is the pathlength through the smoke. As a result, one obtains the calibration functions $K(\lambda, \varphi)$. The final formula for determining the scattering phase function D_{11} and degree of polarization f_{21} of the investigated aerosol from the recorded signals $I^{\mathrm{r}}_{1,2}$ is

$$D^{\mathrm{r}}_{1,2}(\lambda, \varphi) = I^{\mathrm{r}}_{1,2}(\lambda, \varphi)\, K(\lambda, \varphi)/[I_{1,2}(\lambda, \varphi) F_{1,2}(\lambda, \varphi)],$$
$$D_{11}(\lambda, \varphi) = D^{\mathrm{r}}_1 + D^{\mathrm{r}}_2, \qquad (3)$$
$$f_{21}(\lambda, \varphi) = (D^{\mathrm{r}}_1 - D^{\mathrm{r}}_2)/D_{11}.$$

Six analogous signals from three photometers and two signals from the temperature sensors (the temperature of the sampled air and the temperature at the entrance to the working chamber) are fed into the computer interface; the computer interface sends signals for switching the gate, cutoff filter, fluoroplastic screen, and neutral attenuator and low-temperature heater to the control block.

The sequence of operations in the functioning of the device are the following. In the preparatory cycle, zero readings with the gate closed and the signal from the fluoroplastic screen are recorded. In the working cycle, scattering by the sampled air is recorded both with the heater switched off and switched on. The spectral range of the device is $\lambda = 0.4$–0.75 μm, and the wavelength step can be varied by the control program within the limits $\delta\lambda = 5$–50 nm, depending on the specific situation, and the recording time of the two scans varies from 1 to 5 min, depending on the wavelength step.

Discussion of results

It was mentioned above that a quite flexible program was written for controlling the device. This program allows one to record spectral dependences of the components of the scattering matrix in various regimes — from a detailed scan of an arbitrary segment of the spectrum to operational recording at several selected wavelengths within the limits of the entire spectral interval. The latter variant is optimal in studies of the temporal variability of the optical and microphysical characteristics of an aerosol and when the device is working in the regime of field observations. A field test of a prototype of the spectropolarimeter showed[7] that to reconstruct the aerosol particle size distribution and estimate the refractive index of the particle material it is sufficient to measure the polarization components of the scattering phase function D_{11} for three scattering angles at 4–7 wavelengths. The algorithm of the inverse problem is described in Ref. 7. Recall that this algorithm calculates not one kernel but a grid of kernels with different values of the real and imaginary parts of the refractive index, and the unknown parameters n and χ are estimated by running through this grid and finding the kernel that minimizes the error of approximation of the measured quantities. A grid of 45 kernels was calculated in the range of variation of the real part of the refractive index $n = 1.35$–1.59 with a step of 0.03, and of the imaginary part $\chi = 0.0$–0.05 with a step of 0.01.

The algorithm of the inverse problem was validated with the help of a closed mathematical experiment which also estimated the range of particle sizes, information about which is contained in the scattering matrices obtained in the wavelength range 0.4–0.75 μm. It was found to be $r \approx 0.05$–3.0 μm. The errors of reconstruction depended noticeably on the moisture-content of the particles, and varied from 3% for the damp haze to 10% and higher for the dry residue. To unify the measurements in this regime, the entire wavelength range was divided up into seven equal intervals with a step $\Delta\lambda = 50$ nm.

Figures 1*a* and *b* present some results obtained with the help of the spectropolarimeter for the summer

season (May through the beginning of September) of 1993. Spectral dependences of the scattering phase function are shown for φ = 45° and the degree of linear polarization for φ = 45° and φ = 90° under conditions of a dense damp haze (Fig. 1*b*, $S_m \approx 5$ km, $Rh \approx 98\%$) and high transparency (1) (Fig. 1*a*, visibility range $S_m \approx 30$ km, air relative humidity $Rh = 70\%$), i.e., in situations close to limiting.

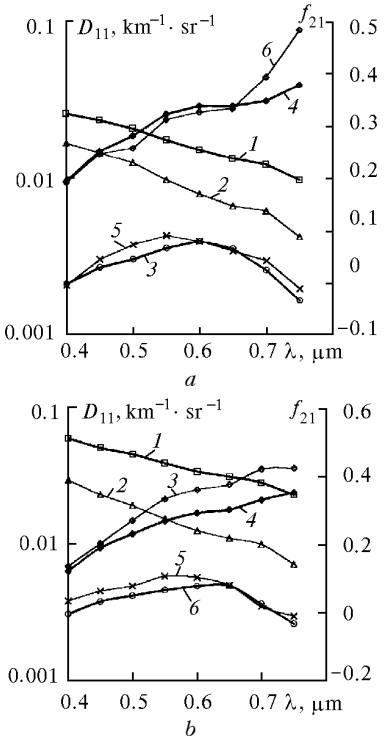

Fig. 1. Spectral dependence of the scattering phase function $D_{11}(\varphi = 45^\circ)$ (curves *1* and *2*) and degrees of linear polarization f_{21} for the angles 45° (*3*, *5*) and 90° (*4*, *6*) for a moist (bold curves) and a dry (solid curves) haze aerosol. Meteorological visibility range $S_m = 30$ km, relative humidity of air $Rh = 70\%$ (*a*). Meteorological visibility range $S_m = 5$ km, relative humidity of air $Rh = 98\%$ (*b*).

Drawbacks of devices with closed working chambers and sampling of the investigated aerosol include moderate heating during sampling. The degree of this heating depends on the air draw-through rate and the difference between the *in situ* temperature and the temperature of the working chamber, which is usually $\Delta T = 0.5$–1°. These distortions are noticeable only for a very high relative humidity ($Rh \approx 100\%$) and have practically no effect for $Rh < 70\%$. For drying of the aerosol by heating, changes in the spectral dependences of its optical characteristics are determined by two often competing processes: an increase in the effective refractive index of the material of the particles and a decrease in their size. "oth of these processes depend on the chemical composition of the particles, and the final result of these competing processes carries information about their chemical composition.

The selection of recorded data presented was chosen to illustrate, among other things, the nonuniqueness of the effect of drying of the aerosol on its optical properties. Curves *1*, *3*, and *4* correspond to *in situ* aerosol, and curves *2*, *5*, and *6* correspond to heater-dried aerosol. In analyzing the results it is natural to focus on peculiarities of the optical characteristics revealed by detailed recording of the spectra. The optics of the aerosol in the visible range of the spectrum (for $\lambda \approx 0.5$ μm) is determined mainly by the mean submicron fraction, which is well described by a log-normal particle size distribution. As one moves into the red region of the spectrum, the relative role of this fraction decreases since scattering by the coarsely dispersed fraction begins to play an increasing role. The number density of this fraction is one to three orders of magnitude smaller than that of the submicron fraction, but the average particle size of this fraction exceeds that of the submicron fraction by roughly the same ratio, and these competing factors should inevitably be manifested in the character of the spectral dependence of the optical characteristics. With growth of the air relative humidity, the role of the submicron fraction becomes noticeably increased due to condensation growth of the particles making up this fraction.

For the model curves the phase function falls monotonically while the degree of linear polarization grows monotonically for both scattering angles. Judging from the deviation from the model dependence, we can say that starting from this wavelength region the defining role shifts over to the coarsely dispersed fraction. The character of the curves in Fig. 1*b* is in qualitative agreement with the behavior of the model curves—$D_{11}(45^\circ)$ and $f_{21}(90^\circ)$ vary monotonically for both the dry and the moist aerosol, only the degree of linear polarization $f_{21}(45^\circ)$ for $\lambda > 0.7$ μm deviates from the model dependence. The nature of the reaction of the polarization curves to desiccation of the particles indicates that their decrease in size predominates over the influence of the refractive index. In Fig. 1*a* deviations from the model dependence show up even in the dependences of D_{11} for $\lambda \approx 0.7$ μm, and in the polarization curves even earlier—for $\lambda \approx 0.55$ μm. The reaction of the polarization curves f_{21} to drying of the particles is almost nil (while for the phase function it is quite large), that is to say, the decrease in the size of the particles is compensated by growth of the refractive index.

On the basis of field measurements of the scattering matrices at the Institute of Atmospheric Physics, an optical model of atmospheric aerosol was constructed,[8] and a microphysical model was then constructed by inverting this model.[9] The matrices were recorded at one wavelength $\lambda = 0.55$ μm; its applicability to other regions of the spectrum in the light of what has been said requires testing and refinement. For the ultraviolet region the model was refined in Ref. 10, where it was shown that the microphysical model of Ref. 9 must be modified

to include the microdispersed fraction. This problem for the red and near-infrared can be solved with the help of the described spectropolarimeter.

For the data of Figs. 1*a*–*b* we solved the inverse problem, i.e., we estimated the refractive index of the material of the particles and reconstructed their size distribution. These distributions are shown in Fig. 2 in the form of dependences of particle volume on size (such a representation affords a more graphic illustration of the fractional structure of the aerosol). Under conditions of a high visibility range the distribution (curve *3*) distinctly separates into a submicron and a coarsely dispersed fraction, separated by a deep minimum near $r \approx 0.8$ μm, but in the range $r = 0.2$–0.8 μm the distribution follows an inverse-power law. With increase in the size of the particles due to an increase in the relative humidity (curve *1*) the submicron fraction shifts toward larger sizes, and the minimum separating the two fractions begins to wash out, with the distribution being well described by an inverse-power law (but more gradual, i.e., with a smaller power) in the range $r = 0.2$–1 μm with the sizes of the more hygroscopic submicron particles dominating throughout this region. Curves *3* and *1* yield the values $n = 1.44$ and $n = 1.35$ for the real part of the refractive index, which is entirely in accord with the physics of the condensation process. Curves *4* and *2* correspond to the dry residue of the aerosol (refractive indices $n = 1.5$ and $n = 1.47$, respectively). It can be clearly seen that with decrease of the relative humidity, the same trend is observed for both the *in situ* aerosol and the dried aerosol, namely the steepness of the falloff of the distribution grows, the coarsely dispersed mode is more clearly delineated, and the refractive index undergoes a noticeable growth. The imaginary part of the refractive index in both cases turned out to be close to zero (less than 0.01).

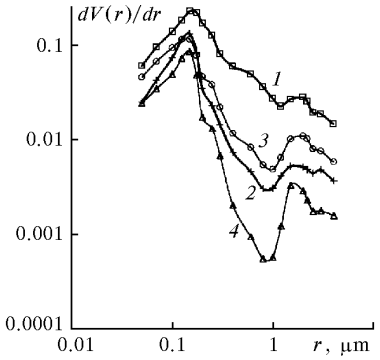

Fig. 2. Examples of particle-volume size distributions reconstructed from the curves shown in Fig. 1: moist aerosol (*1*, *3*), refractive index $n = 1.35$ and 1.44, respectively; dry aerosol (*2*, *4*), $n = 1.47$ and 1.5, respectively.

The presence of simultaneously obtained distributions for the moist aerosol $V_{Rh}(r)$ and the its dry residue $V_d(r)$ allow us to consider the question of the dependence of the condensation activity of the particles on their size. Toward this end, we used a technique analogous to that proposed by A.G. Laktionov.[11] Variations of the particle size distribution density $n(r)$ for variations of the air relative humidity are equivalent to variations of the scale of the radius axis represented by the law $r' = H(r)$ which conserve the integrated number density

$$N = \int_a^b n(r)\mathrm{d}r = N' = \int_{h(a)}^{h(b)} n(h)\mathrm{d}h. \qquad (4)$$

As they condense, the particles move from the size range $[a, b]$ to the size range $[h(a), h(b)]$. Considering N and N' as functions of the upper integration limit, it is possible to seek the dependence $h(r)$, defined in Ref. 11 as the condensation activity of the particles, from the condition $N = N'$. The error associated with the uncertainty in the lower integration limit can be gotten around by integrating $n(r)$ from large radii to small, where the steeply growing N and N' (Fig. 3*a*) very quickly "forget" their initial conditions. The problem reduces to seeking the upper integration limit $r' = h(r)$ from the condition $N = N'$. For the experimental dependences $n(r)$ this invariably leads to one or another form of differentiation of the experimental curve. It would make more sense, in our view, to seek $h(r)$ from smoothed curves using, for example, polynomial interpolation by the method of least squares (MLS). Since the argument and the function are easily interchanged (construction of the inverse problem) in the method of least squares, finding $h(r)$ does not present any difficulty.

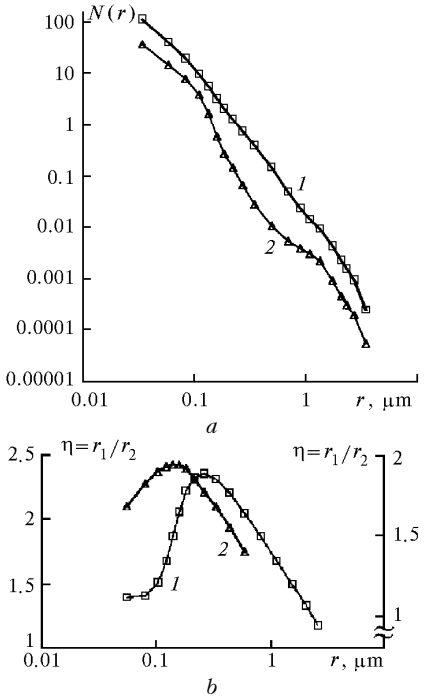

Fig. 3. Total particle number density $N(r)$ for damp haze aerosol of Fig. 1*b* for moist (*1*) aerosol and its dry residue (*2*) (*a*). Dependence on the particle radius r of the condensation activity η of the damp haze sol of Fig. 1*b*, curve *1*, left ordinate axis, and that same dependence calculated in Ref. 11 for the continental aerosol model for relative humidity of air $Rh = 95\%$, curve *2*, right axis (*b*).

Figure 3*a* plots number densities N of a moist aerosol and N' of its dry residue, obtained (without smoothing) from distributions *1* and *2* in Fig. 2 (for a damp haze for relative humidity $Rh = 98\%$). One obtains $n(r)$ from $V(r)$ by dividing by r^3. A quartic polynomial approximated both curves in log–log coordinates with mean-square error around one percent; only individual outliers were noticeably smoothed out. The reconstructed condensation activity η is plotted in Fig. 3*b* (curve *1*) as the ratio of the radius of the moist particle r_1 to that of its dry residue $\eta = r_1/r_2$. Curve *2*, taken from the monograph by Laktionov,[11] illustrates the analogous quantity η calculated by him for model III of continental aerosol and air relative humidity $Rh = 95\%$. In Model III the aerosol is a mixture of completely soluble and completely insoluble particles. The curves are similar in shape, and the absolute values of the maxima of the curves, allowing for the fact that curve *1* was obtained for $Rh \approx 97$–98%, are in good agreement. A noticeable difference is observed only in the position of the maximum on the radius axis. Without going into details, we note that for other realizations the maximum is also observed for large radii, up to $r = 0.4$–0.5 μm. Of course, it cannot be expected that such different methods of estimating the condensation activity will give exactly the same results, and the results of Fig. 3*b* should be seen as indicating at least fair agreement of the estimates; their differences should be the subject of further analysis.

Conclusions

A spectropolarimeter has been built for investigating natural and smoke aerosols, which records the scattering phase function and the degree of linear polarization of the scattered light with quasicontinuous spectral scanning in the wavelength range $\lambda = 0.4$–0.75 μm at which the measurements were made.

In many situations, the spectral dependences of the optical characteristics of natural aerosols in the red spectral range cannot be described using the model of a single-peak distribution; therefore, to extend the optical and microphysical aerosol models developed at the IAF into the red region of the spectrum it is necessary to seriously augment this model.

We have shown that the informative possibilities of the device allow a combined formulation of the inverse problem, namely reconstruction of the particle size distribution and their refractive index. Examples of such a solution are given for a moist aerosol and its dry residue in two different atmospheric situations (high transparency and a dense damp haze).

In the radius interval $r = 0.2$–0.8 μm the reconstructed distributions are well described by an inverse-power law, where the power decreases with growth of the air relative humidity. In the size range $r > 0.8$ μm, even for $Rh \approx 100\%$ a second mode is observed, and with decrease of the relative humidity its contribution to the total volume of the particle grows considerably and on average exceeds 50%.

We have estimated the condensation activity of the particles from the obtained particle size distributions. Its dependence on particle radius has a bell-shaped character with maximum in the region $r = 0.3$–0.4 μm. This result is in good agreement with data obtained with the help of photoelectric counters.

Acknowledgments

In conclusion we thank M.A. Sviridenkov for helpful discussions.

References

1. G.I. Gorchakov, Izv. Akad. Nauk SSSR, Fiz. Atmos. Okeana **9**, No. 2, 204–210 (1973).
2. A.L. Irisov, M.V. Panchenko, et al., in: *Scattering and Refraction of Optical Waves in the Atmosphere* (Institute of Atmospheric Optics, Siberian Branch of the Academy of Sciences of the USSR, Tomsk, 1976), pp. 129–141.
3. V.N. Sidorov, Izv. Akad. Nauk SSSR, Fiz. Atmos. Okeana **15**, No. 7, 763–768 (1979).
4. G.B. Rozenberg, Izv. Akad. Nauk SSSR, Fiz. Atmos. Okeana **12**, No. 11, 1159–1167 (1976).
5. V.S. Kozlov and V.Ya. Fadeev, "*Tables of Optical Characteristics of Light Scattering of a Finely Dispersed Aerosol with Log-Normal Size Distribution*," Preprint No. 31 (Institute of Atmospheric Optics, Siberian Branch of the Academy of Sciences of the USSR, Tomsk, 1981), 64 pp.
6. V.V. Lukshin and A.A. Isakov, Izv. Akad. Nauk SSSR, Fiz. Atmos. Okeana **24**, No. 3, 250–257 (1988).
7. A.A. Isakov, Atmos. Oceanic Opt. **12**, No. 1, 20–27 (1999).
8. G.I. Gorchakov and M.A. Sviridenkov, Izv. Akad. Nauk SSSR, Fiz. Atmos. Okeana **15**, No. 1, 53–59 (1979).
9. G.I. Gorchakov, A.S. Emilenko, and M.A. Sviridenkov, Izv. Akad. Nauk SSSR, Fiz. Atmos. Okeana **17**, No. 1, 39–49 (1981).
10. M.A. Sviridenkov, in: *Proceedings of the Third International Congress on Optical Particle Sizing*, Yokohama (1993), p. 243.
11. A.G. Laktionov, *Equilibrium Heterogeneous Condensation* (Gidrometeoizdat, Leningrad, 1988), 160 pp.
12. M.V. Panchenko and V.Ya. Fadeev, in: *Investigation of Atmospheric Aerosol by Laser Sounding* (Nauka, Novosibirsk, 1980), pp. 202–210.
13. M.V. Panchenko, A.G. Tumakov, and S.A. Terpugova, in: *Apparatus for Remote Sensing of the Parameters of the Atmosphere* (Publishing House of the Tomsk Affiliation of the Siberian Branch of the Academy of Sciences of the USSR, Tomsk, 1987), pp. 40–46.